Comparison of experimental and theoretical fully differential cross sections for single ionization of the 2s and 2p states of Li by O^{8+} ions

Ebrahim Ghanbari-Adivi, Daniel Fischer, Natalia Ferreira, Johannes Goullon, Renate Hubele, Aaron LaForge, Michael Schulz, and Don Madison

Phys. Rev. A **94**, 022715 — Published 30 August 2016

DOI: 10.1103/PhysRevA.94.022715

Comparison of Experimental and Theoretical Fully Differential Cross Sections for Single Ionization of the $2s$ and $2p$ States of Li by O^{8+} Ions

Ebrahim Ghanbari-Adivi[1,2,*] Daniel Fischer[2,3], Natalia Ferreira[3], Johannes Goullon[3], Renate Hubele[3], Aaron LaForge[3], Michael Schulz[1], and Don Madison[1]

[1] *Physics Department and LAMOR, Missouri University of Science and Technology, Rolla, MO USA*

[2] *Department of Physics, Faculty of Sciences, University of Isfahan, Isfahan 81746-73441, Iran*

[3] *Max Planck Institute for Nuclear Physics, Saupfercheckweg 1, 69117 Heidelberg, Germany*

This paper presents a full 3-dimensional (3D) comparison between experiment and theory for 24 MeV O^{8+} single ionization of the $2s$ ground state of lithium and the $2p$ excited state. Two theoretical approximations are examined - the 3-body continuum distorted wave (3DW) and 3-body continuum distorted wave - Eikonal initial state (3DW-EIS). Normally, there is a significant difference between these two approaches and the 3DW-EIS is in much better agreement with experiment. In this case, there is very little difference between the two approaches and both are in very good agreement with experiment. For the excited $2p$ state, the 3D cross sections would exhibit a mirror symmetry about the scattering plane if all 3 magnetic sublevels were excited in equal proportions. For the present experiment, the $2p_{+1}$ ($m = +1$) sublevel is dominantly excited (quantization axis is the incident beam direction) and for this case there is a magnetic dichroism which is observed both experimentally and theoretically.

* ghanbari@phys.ui.ac.ir

I. INTRODUCTION

The importance of studies of atomic collisions in the context of the few-body problem (FBP) has frequently been pointed out [1–4]. The essence of the FBP is that the Schrödinger equation is not analytically solvable for more than two mutually interacting particles even when the underlying forces are precisely known. Therefore, theory has to resort to extensive modelling efforts to obtain numerical solutions and this tends to require very large computational resources. The approximations used in these models have to be tested by detailed experimental data. The most sensitive tests of theory are offered by kinematically complete experiments, in which the momenta of all collision fragments are determined and from which fully differential cross sections (FDCS) can be extracted. A particularly suitable collision reaction to study the FBP is ionization of the target because here the final state involves at least three unbound particles. In contrast, capture or excitation processes kinematically represent two-body scattering processes and, as a result, few-body effects tend to be less pronounced than in ionization.

Since the pioneering work of Ehrhardt *et al.* [5], FDCS measurements have been performed routinely for target ionization by electron impact [3, 5–10] (for a review see e.g. [10]). These studies have led to the development of a large variety of theoretical models ranging from perturbative approaches based on distorted wave methods [11, 12] or methods including final state electron-electron interactions exactly [13–16] to non-perturbative time-independent methods [2, 17, 18] to non-perturbative time-dependent methods [19]. For atomic hydrogen and helium targets, these studies have resulted in major advancements of our understanding of the collision dynamics and these problems can be considered as essentially 'solved'. However, there are still major issues for larger atoms and molecules.

Studying target ionization by ion impact, both experimentally and theoretically, is much more challenging. Kinematically complete experiments are hampered because the large projectile mass results in very small (for fast heavy ion-impact immeasurably small) scattering angles and projectile energy losses (relative to the incident energy). Theoretically, the large projectile mass makes a pure quantum-mechanical treatment of the process very difficult because the description of the projectile requires accounting for an enormous number of angular momentum states of the scattered projectiles. As a result, distorted wave treatments for heavy particles are currently not possible. With the advent of cold target recoil-ion momentum spectroscopy (COLTRIMS) [20, 21], also known as reaction microscopes (ReMi), kinematically complete experiments for ion-impact ionization became feasible [22–28] (for a review see [28]). These measurements sparked significant theoretical activities as well. Initially, these studies were restricted to perturbative methods [29–36], but more recently non-perturbative calculations were reported [37–39].

Given the experimental and theoretical challenges in studying ionization by ion impact, it is not surprising that our understanding of the few-body dynamics is significantly less complete than for electron impact. Part of the discrepancies between experiment and theory can be associated with the projectile coherence properties [40–43], which were not accounted for in theoretical models until recently and which have an insignificant effect on cross sections for electron impact. In addition, for highly charged ions, higher-order contributions are much stronger than for electron impact and also contribute to larger discrepancies between experiment and theory. Finally, the experimental resolution, which tends to be somewhat worse than for electron impact, complicates the comparison to theory.

Another limitation of kinematically complete experiments for ion impact is that only a small variety of target species are accessible. COLTRIMS is only feasible for gaseous targets of relatively small mass number because the momentum resolution gets worse with increasing mass. These limitations were overcome with the recent development of MOTReMi [44]. In this device a magneto-optical trap (MOT), providing a very cold target and thereby improving the overall momentum resolution by about a factor of 3, is combined with a ReMi. With this apparatus, kinematically

complete experiments for ion impact ionization of targets other than helium and molecular hydrogen, namely for lithium, became feasible. Previously, double differential ejected electron spectra were reported [45, 46], but using the new MOTReMi apparatus FDCS were measured for the first time [47].

There are several features offered by a lithium target which lead to qualitative differences to helium in the collision dynamics. First of all, the radial nodal structure of the ground state wavefunction of the valence electron ($2s$) leads to richer structures in the FDCS. Second, the valence shell contains only a single electron and the inner shell is far away from the valence shell, both spatially and energetically. As a result, electron-electron correlation effects are expected to be much less important than in helium. Finally, a significant fraction of the target atoms gets excited to the $2p$ state in the field of the cooling laser. Due to the magnetic field of the trap, this excited state is Zeeman-split and the energetically lowest lying Zeeman state ($m = \pm 1$ depending on the polarization of the magnetic field) is predominantly populated. As a result, the target is spin-polarized, which leads to asymmetries in the FDCS for $2p$ ionization, also known as magnetic dichroism (or sometimes called orientational dichroism).

It is certainly of considerable interest to understand to what extent the few-body dynamics is affected by these features. However, the experimental data for a lithium target were only recently reported. As a result, theoretical studies have also recently started to shift focus from helium to lithium [47–52]. In this article, we present a comprehensive comparison between experiment and theory covering a broad range of kinematic parameters for ionization both from the ground state and from the $2p$ state. Some fully differential cross sections obtained from the same experimental run were presented in Schultz *et al.* [26] and Hubele *et al.* [47]. In [26], the post-collision interaction in $2s$ ionization of lithium was studied for the FDCS in the scattering plane. In [47], experiment was compared to theory for two cases in a plane perpendicular to the incident beam direction. Here, we compare experiment and theory for the full 3-dimensional cross section for three cases and for each case examine results in both the scattering plane and perpendicular plane (also sometimes called the azimuthal plane).

II. EXPERIMENT

The experiment was performed with the magneto-optical trap reaction microscope MOTReMi [44, 53] implemented in the ion storage ring TSR at the Max-Planck Institute for Nuclear Physics in Heidelberg (MPI). The O^{8+} ions were created and accelerated to an energy of 1.5 MeV/amu using the MPI tandem accelerator. The ion beam was injected in the storage ring, cooled in the TSR electron cooler, and bunched with the TSR RF cavity with bunch durations of few ns and a repetition rate of about 3 MHz. In the MOTReMi, the ion beam was intersected with a laser-cooled atomic lithium cloud. After an ionization event, electrons and lithium ions are extracted towards two detectors in opposite directions by the combination of an electric (0.6 V/cm) and a homogenous magnetic field (7.7 Gauss). Their measured time-of-flight and their position on the detector are used to calculate the particles' momenta.

As compared to conventional experiments with ground-state atoms prepared in a gas-jet, there are essentially two complications due to the operation of the magneto-optical trap (MOT) and the study of optically excited target atoms: First, the MOT requires an inhomogeneous magnetic field for the trapping of the atoms which renders the momentum-resolved detection of electrons in the reaction microscope impossible. Second, the (incoherent) optical excitation leads to a mixture of ground ($2s$) and excited ($2p$) state target atoms. Furthermore, this excitation can never result in an excited state population exceeding 50%, so that neither a pure ground state nor a pure excited state can be achieved while the target atoms are exposed to the cooling laser light. In this experiment the excited state population was around 20%.

Both challenges are mastered by employing a sophisticated switching cycle of the MOT magnetic field and the cooling lasers. First, the MOT magnetic field is periodically switched off for a few milliseconds. During this measurement period, the atoms are stilled located in the trap region and emitted electrons can easily be momentum-analyzed. Second, the cooling lasers are also switched off, but only for a duration of a couple of hundred microseconds. In this period, all the target atoms are in the $2s$ ground state (the excited $2p$ state has a lifetime of only about 27 ns). Cross sections for excited state ionization can be obtained by subtracting the measured spectra for the periods with the laser beams being switch on (providing the target in a $2p$-$2s$ mixture) and switched off (providing a pure $2s$ target). The spectrum for the laser beams switched on has to be weighted with consideration of the excited state population of 20% (see e.g. LaForge et. al. [54]).

It should be noted that there is a strong asymmetry in the population of the magnetic sub-levels of the excited $2p$ state while the cooling lasers are switched on. This is due to the homogenous magnetic field of the reaction microscope applied to extract the collision fragments. The Zeeman splitting of the excited $2p$ state along with a red-detuning of the laser light from the $2s$-$2p$ resonance results in the predominant population of the magnetic sub-levels with lower energy (in the present case $m = +1$). We estimate a population of 0.86, 0.09, and 0.05 for the magnetic sub-states with m =+1, 0, and -1, respectively. A higher degree of polarization can be obtained by employing optical pumping [53], however, this technique was not used in the experiment described here.

III. THEORETICAL MODELS

The two theoretical models considered here are the three-body distorted wave (3DW) approximation and the three-body distorted wave-Eikonal initial state (3DW-EIS) approximation. The details of these approaches can be found in [33, 55, 56] so only a brief overview will be given here. These two models are very similar and the only difference is the initial-state wavefunction for the incoming projectile.

To reduce the complexity of the few-body problem, we consider the outer-shell electron as the active electron and assume that the other electrons are frozen in their initial states during the collision process. Consequently, the scattering process can be treated as a three-body problem. The effects of the passive electrons are taken into account in the calculation of the effective potential seen by the ejected electron (the distorting potential).

Let's consider a typical three-body collision system in which the projectile P impinges on the initially bound target ion (i.e. the target atom without the active electron) plus electron ($T + e$) subsystem and causes the ejection of the electron e. In the 3DW approximation, the initial state of the scattering system is approximated as

$$\Phi_i^+(\mathbf{r}, \mathbf{R}) = \varphi_i(\mathbf{r}) \exp(i\mathbf{K}_i \cdot \mathbf{R}), \tag{1}$$

where $\varphi_i(\mathbf{r})$ is the initial bound state for the active electron which is calculated using the usual self-consistent Hartree-Fock method. The projectile wavefunction is a plane wave with initial momentum $\mathbf{K}_i$ and $(\mathbf{r}, \mathbf{R})$ are the position vectors of e and P with respect to the target nucleus. The exact final state is approximated as

$$\Psi_f^-(\mathbf{r}, \mathbf{R}) = \chi_e^-(\mathbf{r}) C_P^-(\mathbf{K}_f, \mathbf{R}) D_{Pe}(\mathbf{r}, \mathbf{R}) \tag{2}$$

where $\chi_e^-(\mathbf{r})$ is the continuum state of the ejected electron in the field of the target ion T, $C_P^-(\mathbf{K}_f, \mathbf{R})$ is a Coulomb wave for P in the field of T with momentum $\mathbf{K}_f$, and $D_{Pe}(\mathbf{r}, \mathbf{R})$ is a function that takes into account the Coulomb interaction between the projectile and the ejected electron (post-collision interaction PCI). The ejected-electron wavefunction $\chi_e^-(\mathbf{r})$, called a distorted wave, is a numerical solution of the Schrödinger equation

$$(T_e + U_f - E_e)\chi_e^-(\mathbf{r}) = 0, \tag{3}$$

where T_e is the kinetic energy operator for the electron, the distorting potential U_f is a spherically symmetric potential for the T-e interaction which is calculated using the Hartree-Fock charge density for the final state ion, and E_e is the energy of the ejected electron. With these approximations, the 3DW T-matrix is

$$T_{fi}^{3DW} = \int d\mathbf{r}d\mathbf{R}\Psi_f^{-*}(\mathbf{r},\mathbf{R})V_i(\mathbf{r},\mathbf{R})\Phi_i^+(\mathbf{r},\mathbf{R}), \tag{4}$$

where $V_i(\mathbf{r},\mathbf{R})$ is the Coulomb P-e interaction. This 6-dimensional integral is evaluated numerically.

In a second approach, the exact two-potential form of the transition amplitude first derived by Gell-Mann and Goldberger [57]

$$T_{fi} = \langle\Psi_f^-|W_f^\dagger|\Psi_i^+\rangle + \langle\Psi_f^-|V_i - W_f^\dagger|\Phi_i^+\rangle \tag{5}$$

is used, in which Ψ_i^+ is the exact initial state wavefunction, Φ_i^+ is the asymptotic initial state wavefunction of Eq. (1), Ψ_f^- is an approximate final state wave function (we use the same one as Eq. (2)) which determines the final state perturbation W_f. If we approximate Ψ_i^+ as Φ_i^+, the above exact amplitude reduces to the 3DW transition amplitude. However, Crothers [58] and Crothers and McCann [29] showed that a better approximation for Ψ_i^+ is to use an Eikonal wave function which satisfies the correct boundary conditions. This approximation was called the CDW-EIS (coulomb distorted wave - Eikonal initial state). In this approach, an analytical Coulomb wave is used for the ejected electron whereas we use a numerical distorted wave for the ejected electron so we call our approximation 3DW-EIS (3-body distorted wave - Eikonal initial state). The final state perturbation potential is given by

$$W_f(\mathbf{r},\mathbf{R}) = \frac{1}{\Psi_f^-(\mathbf{r},\mathbf{R})}(H-E)\Psi_f^-(\mathbf{r},\mathbf{R}). \tag{6}$$

Here H is the total Hamiltonian and E is the total energy of the system. In order to obtain an analytic expression for the perturbation, we assume that the ejected electron wavefunction is a Coulomb wave with an effective charge of $+1$. The full expression for the latter case can be found in Jones and Madison [59]. The Eikonal initial state wave function is given by

$$\Psi_i^+ \approx \Psi_i^{EIS}(\mathbf{r},\mathbf{R}) = \Phi_i^+(\mathbf{r},\mathbf{R})\exp\left[i\frac{Z_P}{\mathrm{v}_i}\ln[\frac{\mathrm{v}_i R - \mathbf{v}_i\cdot\mathbf{R}}{\mathrm{v}_i|\mathbf{R}-\mathbf{r}| - \mathbf{v}_i\cdot(\mathbf{R}-\mathbf{r})}\right], \tag{7}$$

where $\mathbf{v}_i$ is the velocity of the projectile with respect to the target.

The fully differential cross section (FDCS) for scattering of the projectile into solid angle $d\Omega_P$ and ejection of the electron into solid angle $d\Omega_e$ is given by [33, 55]

$$\frac{d^3\sigma}{d\Omega_P d\Omega_e dE_e} = (2\pi)^4 N_e \mu_{Te}\mu_i^2 k_e K_f K_i |T_{fi}|^2, \tag{8}$$

in which μ_i is the initial reduced mass of the whole system, μ_{Te} is the reduced mass of the subsystem $(T+e)$ and N_e is the number of the electrons equivalent to the active electron in the target.

In the paper of Hubele *et al.* [47], experiment was compared with a CDW-EIS calculation which is a similar calculation. The differences between these two calculations are the following: (1) The CDW-EIS approach uses a semi-classical straight line approach for the projectile while our approach is fully quantum mechanical. (2) For the active electron, we use a Hartree-Fock bound state wavefunction and a numerical distorted wave for the continuum electron. (3) Standard CDW-EIS calculations only evaluate the first term of Eq. (5) while we evaluate both terms.

IV. RESULTS

In this section the theoretical and experimental results are presented and compared. The coordinate system we are using has the z-axis in the incident beam direction and the xz plane is the scattering plane with the projectile

being scattered in the direction of the $+x$ axis. This means that the transverse momentum transfer direction is in the $-x$ direction. Figure 1 compares three-dimensional images of 3DW-EIS results and experiment for the FDCS for ionization of the $2s$ and $2p$ states of lithium atoms by impact of bare oxygen ions with an incident energy of 24 MeV. The projectile momentum transfer is defined as $\mathbf{q} = \mathbf{K}_i - \mathbf{K}_f$ and along with $\mathbf{K}_i$ it spans the scattering plane. For $2s$ states, q and the ejected electron energy (E_e) are $q = 1$ au and $E_e = 1.5$ eV. For ionization of the $2p$ states, two sets of these values are considered: (q =0.3 au, E_e =1.5 eV) and (q =0.4 au, E_e=3 eV).

There are two features which are normally seen in the FDCS for single ionization of the target which are often described in terms of classical mechanisms. In the first, the projectile knocks the active atomic electron into its final state while the residual ion remains as a spectator. The electron emission occurs nearly in the same direction as $\mathbf{q}$ and the cross sections normally have a peak near this direction which is called the binary peak. In the second, the collision of the active electron with the projectile is followed by a backscattering of the electron from the target core. In this mechanism, the electron ejection is nearly into the opposite direction of $\mathbf{q}$ and the peak near this direction is called the recoil peak. Normally, it is expected that these mechanisms will lead to a double-peak structure both in experimental and theoretical results for the FDCSs. From Fig. 1, we can see that the $2s$ results have a binary peak (large round peak to the right) and recoil peak (smaller wing-like feature to the left). However, there is almost no recoil peak for the two $2p$ cases.

As is seen, there is reasonable good agreement between the theoretical calculations and experiment in general. The binary peak is completely dominant for all cases. The interesting experimental and theoretical $2s$ recoil wings are very similar, while these wings are absent in the images for the $2p$ electrons. Hubele *et al.* [47] as well as Walters and Whelan [50] have suggested that the wings are due to the nodal structure of the initial $2s$ state along with the interaction between the projectile and target nucleus - the so called nucleus-nucleus (NN) interaction. On the other hand, Gulyás *et al.* [51] found that the wings resulted from the NN interaction plus a binary collision.

The next set of figures show planar slices through the 3D plots. Figure 2 compares experimental and theoretical FDCSs for ejection of $2s$ and $2p$ electrons into the scattering plane. The angle θ_b is the ejected electron observation angle measured clockwise in the scattering plane relative to $\mathbf{K}_i$ and the maximum cross sections are at 90° which is close to the momentum transfer direction. For each case, the projectile momentum transfer and ejected electron energy are the same as in Fig. 1. The experimental and theoretical results are both normalized to unity at the binary peak ($\theta_b = 90°$). Both experiment and theory exhibit the same characteristic shape - a pronounced binary peak and almost no recoil peak. This observation shows the value of 3D plots. In Fig. 2, the slice selecting the scattering plane reduces this extended 'recoil ring' to a narrow feature of relatively small intensity. Therefore, in the 3D plot, the recoil structure is much easier to see because it systematically spans a broad range of electron emission planes. In all cases, the 3DW and 3DW-EIS approaches predict nearly the same values for the cross sections. Typically, EIS results are significantly better than the 3DW incident plane wave results, but that is obviously not the case here which suggests that the initial state interaction between the projectile and target is apparently not very important at least in terms of the projectile wavefunction.

Overall, the agreement between experiment and theory is reasonably good. The largest difference between theory and experiment is seen for the $2s$ state where theory underestimates the left side of the binary peak and overestimates the right side, (there is also a right side overestimation for $2p$ (q=0.3 au, E_e=1.5 eV) case). The best agreement is found for the $2p$ state with q=0.4 au, E_e=3 eV case and there a very good agreement for the small structure appearing in the cross sections for ionization in the angular region to the left of the binary peak.

The FDCSs for single ionization of lithium are displayed in Fig. 3 for the electrons emitted into the plane perpendicular to the incident beam direction which we will call the perpendicular plane (it has also been called the azimuthal

plane). The kinematic parameters for which the FDCS are displayed and the normalization of the data are the same as for the previous figures. We use standard spherical coordinates with the azimuthal angle φ_b being measured relative to the x-axis. As a result, the binary peak in the $-x$ direction occurs for $\varphi_b = 180°$. In the original paper of Hubele *et al.* [47], φ_b was measured relative to the positive y-axis and the binary peak occurs for $\varphi_b = 90°$. Again the overall agreement between experiment and theory is reasonably good with only small differences between experiment and theory for most of the scattering angles. The triple peak structure for the $2s$ state with a deep minimum results from the two symmetric wings seen in the 3D view of Fig. 1. The largest difference between experiment and theory is seen for ionization of the $2s$ state where the magnitude of the side wings in underestimated by theory. For the $2s$ case, the experimental data exhibits mirror symmetry with respect to 180° (scattering plane).

For the $2p$ case, there is only a single, much broader peak than in the $2s$ case and the mirror symmetry is broken. Both experiment and theory have peak maxima shifted to angles larger than 180° and the peak maxima are larger than unity in our normalization (i.e. the cross section for the momentum transfer in the scattering plane is not the maximum cross section). Again the agreement is best for the $2p$ case with q=0.4 au and E_e=3 eV. The breaking of the mirror symmetry with respect to the scattering plane is due to the polarization of the initial target state which is called magnetic dichroism [47, 60]. It is seen that both the 3DW and 3DW-EIS theories give a good description of dichroism for ionization from the initial $2p$ states.

There would be no dichroism if both the $2p_{+1}$ and $2p_{-1}$ substates contributed equally to the ionization cross section. For the present experiment, the relative contributions of the cross sections were 86% $2p_{+1}$, 9% $2p_0$, and 5% $2p_{-1}$ (the quantization axis is the direction of the beam axis). In Fig. 4, the individual $2p_{+1}$ and $2p_{-1}$ substate theoretical 3DW-EIS cross sections are compared with experiment for the same previous values of q and E_e. The normalized results are obtained using the 3DW-EIS approach for ionization in the perpendicular plane and shown as a function of the ejected electron angle. As has been discussed by Walters and Whelan [50], the FDCS for $m = +1$ is the mirror image of that for $m = -1$ relative to the scattering plane (i.e. $\theta_b = 180°$). The $m = 0$ substate cross sections are symmetric about the scattering plane but the dominant contribution of the $2p_{+1}$ substate yields a cross sections that is not symmetric with respect to the scattering plane, and the resulting theoretical $2p$ ionization cross sections show the magnetic dichroism in accordance with the experimental findings.

There have been three previously published theoretical calculations for two of the perpendicular plane cases. There were CDW-EIS results shown in the original Hubele *et al.* [47] paper, later Gulyás *et al.* [51] used the CDW-EIS method to make a detailed study of the 2s wings using three different models for the effective nuclear-nuclear (NN) interaction, and Walters and Whelan [50] reported a coupled pseudostate calculation (CP). Figure 5 shows a comparison of the present results with the previous calculations. The Gulyás *et al.* [51] results are the ones that used the polarization approximation of Eq. (6) in that paper which gave the best agreement with experiment for the doubly differential cross sections. It is seen that the results are all pretty similar. For $2s$ ionization, the best overall agreement with experiment is probably the CP results of Walters and Whelan [50] although the Gulyás *et al.* [51] results are also very good. For ionization of the $2p$ state, the 3DW-EIS results are probably in the best overall agreement with experiment. The other theoretical approaches predict the magnitude of the $2s$ side peaks much better than the 3DW-EIS while the 3DW-EIS does a little better job of predicting the width of the central $2s$ peak and the $2p$ peak.

There has been a fairly extensive discussion about what causes the $2s$ wings. As mentioned above, Hubele *et al.* [47] and Walters and Whelan [50] have attributed the wings to the NN interaction and the double nodal structure of the 2s wavefunction. On the other hand, Gulyás *et al.* [51] have attributed the wings to a combination of the NN interaction and a binary interaction. In the CDW-EIS approach, the NN interaction is included through an overall phase factor containing the NN interaction. The 3DW-EIS also has the NN interaction in the Eikonal phase of Eq. (7) where the

screened nucleus is approximated as a particle of charge +1. Since we are treating the projectile as a wavefunction, the Eikonal phase is part of the integral and cannot be taken out as an overall phase factor. In the present results, it is clear that the NN interaction in the Eikonal phase is not responsible for the side wings since we get them using a plane wave which has no NN contributions. We can put in an approximate NN interaction by adding a nuclear potential (V_{nuc}) to the initial state interaction V_i (the perturbation) in Eq. (4),

$$V_i = V_{Pe} + V_{nuc}, \tag{9}$$

where V_{Pe} is the $P - e$ interaction potential. We would note that V_{nuc} only depends on the projectile coordinate and a single particle potential which only depends on the projectile coordinates would not contribute to a Born type calculation due to the orthogonality of the bound and continuum wavefunctions for the ejected electron. The 3DW-EIS approach does not have this orthogonality due to the ejected electron coordinates in the final state Coulomb interaction between the ejected electron and projectile. The simplest approximation for V_{nuc} would be to treat the nucleus plus two electrons as a single proton as is done in the Eikonal phase. We will call this approximation V_{ion}. A better approximation would be to use a screened potential which has an effective charge of three at the origin and an asymptotic charge of unity. We have used the effective potential of Green, Sellin, and Zachor [61–63] known as the GSZ potential. The explicit form of this potential is given by

$$V_{GSZ}(R) = \frac{Z_P(Z_T - n)[1 - \Omega(R)]}{R}, \tag{10}$$

where $n + 1$ is the number of the electrons in the atom or ion and

$$\Omega(R) = \frac{1}{1 - \frac{\eta}{\beta}[1 - \exp(\beta R)]}, \tag{11}$$

with η and β as two adjustable parameters and Z_P and Z_T the number of protons in the projectile and target core. For lithium, $\eta = 1.75$ and $\beta = 2.165$. Figure 6 compares 3DW-EIS results with no NN interaction in the perturbation to calculations using V_{ion} and V_{nuc}. It is seen that adding the NN interaction to the perturbation significantly increases the magnitude of the side wing peak. The V_{ion} results are very similar to those of Hubele *et al.* [47]. It is also seen that the width of the central peak becomes more narrow which is also similar to the other theoretical calculations and in worse agreement with experiment. It is interesting that the presumably better screened nuclear treatment is in the worst agreement with experiment. The large sensitivity to the screening is also surprising since it would appear that it should be a small effect. For example, the effective charge is 3.00 at the origin, 1.28 at $R = 1$ au , 1.03 at $R = 2$ au, and 1.00 at $R = 3$ au, so it deviates from unity only in a very small region of space.

We also investigated the source of the wings we get without having a NN term in the perturbation. Typically, CDW-EIS calculations use Coulomb waves for the ejected electron so we tried that. In Fig. 7, 3DW-EIS results calculated using a distorted wave for the ejected electron are compared with a completely equivalent calculation using Coulomb waves. It is seen that the side wings are greatly reduced. This calls the attention for the importance of the more realistic description of the ejected electron using screened potential. To check the effect of the double nodal wavefunction, we performed a completely equivalent 3DW-EIS calculation except we used a $1s$ wavefunction instead of $2s$ and those results are also shown in Fig. 7. It is seen that the wings are completely gone. Consequently, our results support the conclusions of Hubele *et al.* [47] and Walters and Whelan [50] attributing the wings to the NN interaction and the double nodal structure of the $2s$ wavefunction. However, we find that the NN interaction is important in the perturbation and not in the Eikonal phase and we also find an additional enhancement to the wings from using a screened potential for the calculation of the ejected electron wavefunction.

V. CONCLUSIONS

We have presented a full 3D comparison between experiment and theory for 24 MeV O^{8+} single ionization of the $2s$ ground state of lithium and the $2p$ excited state. Two theoretical approximations were examined -the 3-body continuum distorted wave (3DW) and 3-body continuum distorted wave - Eikonal initial state (3DW-EIS). The difference between these two calculations is that the 3DW-EIS uses an Eikonal approximation for the incident projectile wavefunction and the 3DW uses a plane wave. In the 3D images for ionization of the $2s$ state, a prominent binary peak was seen and a recoil peak which had an interesting wing-type structure. In the 3D images for ionization of the $2p$ state, a prominent binary peak was seen and essentially no recoil peak. Normally, there is a significant difference between the 3DW and 3DW-EIS results and 3DW-EIS is in much better agreement with experiment. In this case, there is very little difference between the two approaches and both are in very good agreement with experiment. For ionization of the $2s$ state, the 3D images have a mirror symmetry about the scattering plane while for ionization of the $2p$ state, this symmetry is broken. The $2p$ state would have mirror symmetry if the $2p_{-1}$ and $2p_{+1}$ substates were excited in equal proportions. For the present experiment, the $2p_{+1}$ sublevel is dominantly excited (quantization axis is the incident beam direction) and for this case there is a magnetic dichroism which is observed both experimentally and theoretically.

There were three previous theoretical calculations - two CDW-EIS (continuum distorted wave - Eikonal initial state calculations by Hubele *et al.* [47] and Gulyás *et al.* [51] and a coupled pseudostate (CP) calculation of Walters and Whelan [50] for the perpendicular plane only and we compared with these results as well. We found that the Walters and Whelan and Gulyas *et al.* results gave the best agreement with experiment for the $2s$ state while the 3DW-EIS results were in the best overall agreement for the $2p$ state. The 3DW-EIS predicted the central width a little better for both the $2s$ and $2p$ states.

There has been considerable discussion about the source of the $2s$ wings. Hubele *et al.* [47] and Walters and Whelan [50] have attributed the wings to the NN interaction and the double nodal structure of the $2s$ wavefunction. Gulyás *et al.* [51] have attributed the wings to a combination of the NN interaction and a binary interaction. All three of those calculations use the semi-classical straight line approximation for the projectile. We use a full quantum mechanical wave treatment for the projectile and we get wings even if the NN interaction is neglected for the incident projectile wavefunction. However, the wings were greatly enhanced if we added a NN interaction to the initial state perturbation. We found that the wings we get go away if we neglect NN in the perturbation, use a Coulomb wave for the ejected electron and use a $1s$ wavefunction for the ejected electron. Consequently, while our results support the wings resulting from the NN interaction and the double nodal structure of the $2s$ wavefunction, we find an additional enhancement from using a screened potential for the calculation of the ejected electron wavefunction.

ACKNOWLEDGMENTS

DM and MS would like to acknowledge the support of the US National Science Foundation under Grant. Nos. PHY-1505819 and PHY-1401586, respectively. EGA would like to acknowledge sabbatical support provided by Missouri S&T and the University of Isfahan. DF was supported by an Emmi Noether grant from the German Research

Foundation under grant No. FI 1593/1-1.

[1] M. Schulz, R. Moshammer, D. Fischer, H. Kollmus, D. H. Madison, S. Jones, and J. Ullrich, Nature **422**, 48 (2003)
[2] T. N. Rescigno, M. Baertschy, W. A. Isaacs and C. W. McCurdy, Science **286**, 2474 (1999)
[3] A. Lahmann-Bennani, J. Phys. B: At. Mol. Opt. Phys. **24**, 2401 (1991)
[4] M. Schulz and D. H. Madison, Int. J. Mod. Phys. A **21**, 3649 (2006)
[5] H. Ehrhardt, M. Schulz, T. Tekaat, and K. Willmann, Phys. Rev. Lett. **22**, 89 (1969)
[6] J. RÖder, H. Ehrhardt, I. Bray, D. V. Fursa , I. E. McCarthy, J. Phys. B: At. Mol. Opt. Phys. **29**, 2103 (1996)
[7] A. J. Murray, M. B. J. Woolf, and F. H. Read, J. Phys. B: At. Mol. Opt. Phys. **25**, 3021 (1992)
[8] G. Stefani, L. Avaldi, and R. Camilloni, J. Phys. B: At. Mol. Opt. Phys. **23**, L227 (1990)
[9] A. Dorn, R. Moshammer, C. D. Schröter, T. J. M. Zouros, W. Schmitt, H. Kollmus, R. Mann, and J. Ullrich, Phys. Rev. Lett. **82**, 2496 (1999)
[10] M. A. Haynes and B. Lohmann, J. Phys. B: At. Mol. Opt. Phys. **33**, 4711 (2000)
[11] D. H. Madison, R. V. Calhoun, and W. N. Shelton, Phys. Rev. A **16**, 552 (1977)
[12] C. T. Whelan, and H. R. J. Walters, J. Phys. B: At. Mol. Opt. Phys. **23**, 2989 (1990)
[13] M. Brauner, J. S. Briggs, and H. Klar, J. Phys. B: At. Mol. Opt. Phys. **22**, 2265 (1989)
[14] A. Prideaux, D. H. Madison and K. Bartschat, Phys. Rev. A **72**, 032702 (2005)
[15] B. Joulakian, C. Dal Cappello, and M. Brauner, J. Phys. B: At. Mol. Opt. Phys. **25** 2863 (1992)
[16] D. H. Madison and O. Al-Hagan, J. At. Mol. Phys. **2010**, 367180 (2010)
[17] K. Bartschat, and P. G. Burke, J. Phys. B: At. Mol. Opt. Phys. **20**, 3191 (1987)
[18] I. Bray, D. V. Fursa, Phys. Rev. Lett. **76**, 2674 (1996)
[19] J. Colgan, M. S. Pindzola, F. J. Robicheaux, D. C. Griffin, and M. Baertschy, Phys. Rev. A **65**, 042721 (2002)
[20] R. Dörner, V. Mergel, O. Jagutzki, L. Spielberger, J. Ullrich, R. Moshammer, and H. Schmidt-Böcking, Phys. Rep. **330**, 95 (2000)
[21] J. Ullrich, R. Moshammer, A. Dorn, R. Dörner, L. Ph. H. Schmidt, and H. Schmidt-Böcking, Rep. Prog. Phys. **66**, 1463 (2003)
[22] N. V. Maydanyuk, A. Hasan, M. Foster, B. Tooke, E. Nanni, D. H. Madison, and M. Schulz, Phys. Rev. Lett. **94**, 243201 (2005)
[23] M. Schulz, R. Moshammer, A. N. Perumal, and J. Ullrich, J. Phys. B: At. Mol. Opt. Phys. **35**, L161 (2002)
[24] M. Schulz, R. Moshammer, A. Voitkiv, B. Najjari, and J. Ullrich, Nucl. Instrum. Meth. B **235**, 296 (2005)
[25] D. Fischer, R. Moshammer, M. Schulz, A. Voitkiv, and J. Ullrich, J. Phys. B: At. Mol. Opt. Phys. **36**, 3555 (2003)
[26] M. Schulz, B. Najjari, A. B. Voitkiv, K. Schneider, X. Wang, A. C. Laforge, R. Hubele, J. Goullon, N. Ferreira, A. Kelkar, M. Grieser, R. Moshammer, J. Ullrich, and D. Fischer, Phys. Rev. A **88**, 022704 (2013)
[27] A. Hasan, S. Sharma, T. P. Arthanayaka, B. R. Lamichhane, J. Remolina, S. Akula, D. H. Madison, and M. Schulz, J. Phys. B: At. Mol. Opt. Phys. **47**, 215201 (2014)
[28] A. Hasan, T. Arthanayaka, B. R. Lamichhane, S. Sharma, S. Gurung, J. Remolina, S. Akula, D. H. Madison, M. F. Ciappina, R. D. Rivarola, and M. Schulz, J. Phys. B: At. Mol. Opt. Phys. **49**, 04LT01 (2016)
[29] D. S. F. Crothers, and J. F. McCann, J. Phys. B: At. Mol. Phys. **16**, 3229 (1983)
[30] D. H. Madison, M. Schulz, S. Jones, M. Foster, R. Moshammer, and J, Ullrich, J. Phys. B: At. Mol. Opt. Phys. **35**, 3297 (2002)
[31] A. B. Voitkiv, B. Najjari, and J. Ullrich, J. Phys. B: At. Mol. Opt. Phys. **36**, 2591 (2003)
[32] M. F. Ciappina, W. R. Cravero, and C. R. Garibotti, J. Phys. B: At. Mol. Opt. Phys. **36**, 3775 (2003)
[33] M. Foster, D. H. Madison, J. L. Peacher, M. Schulz, S. Jones, D. Fischer, R. Moshammer, and J. Ullrich, J. Phys. B: At.

Mol. Opt. Phys. B **37**, 1565 (2004)

[34] K. A. Kouzakov, S. A. Zaytsev, Y. V. Popov, and M. Takahashi, Phys. Rev. A **86**, 032710 (2012)

[35] X. Y. Ma, X. Li, S. Y. Sun, and X. F. Jia, Europhys. Lett. **98**, 53001 (2012)

[36] E. Ghanbari-Adivi, and S. Eskandari, Chin. Phys. B **24**, 103403 (2015)

[37] J. Colgan, M. S. Pindzola, F. Robicheaux, and M. F. Ciappina, J. Phys. B: At. Mol. Opt. Phys. **44**, 175205 (2011)

[38] H. R. J. Walters, and C. T. Whelan, Phys. Rev. A **85**, 062701 (2012)

[39] H. R. J. Walters, and C. T. Whelan, Phys. Rev. A **92**, 062712 (2015)

[40] K. N. Egodapitiya, S. Sharma S, A. Hasan, A. C. Laforge, D. H. Madison, R. Moshammer, and M. Schulz, Phys. Rev. Lett. **106**, 153202 (2011)

[41] X. Wang, K. Schneider, A. LaForge, A. Kelkar, M. Grieser, R. Moshammer, J. Ullrich, M. Schulz, D. Fischer, J. Phys. B: At. Mol. Opt. Phys. **45**, 211001 (2012)

[42] S. Sharma, T. P. Arthanayaka, A. Hasan, B. R. Lamichhane, J. Remolina, A. Smith, and M. Schulz, Phys. Rev. A **90**, 052710 (2014)

[43] L. Sarkadi, I. Fabre, F. Navarrete, and R. O. Barrachina, Phys. Rev. A **93**, 032702 (2016)

[44] D. Fischer, D. Globig, J. Goullon, M. Grieser, R. Hubele, V. L. B. de Jesus, A. Kelkar, A. LaForge, H. Lindenblatt, D. Misra, B. Najjari, K. Schneider, M. Schulz, M. Sell, and X. Wang, Phys. Rev. Lett. **109**, 113202 (2012)

[45] N. Stolterfoht, J.-Y. Chesnel, M. Grether, B. Skogvall, F. Frémont, D. Lecler, D. Hennecart, X. Husson, J. P. Grandin, B. Sulik, Gulyás, and J. A. Tanis, Phys. Rev. Lett. **80**, 4649 (1998)

[46] J. A. Tanis, J.-Y. Chesnel, F. Fremont, D. Hennecart, X. Husson, A. Cassimi, J. P. Grandin, B. Skogvall, B. Sulik, J.-H. Bremer, and N. Stolterfoht, Phys. Rev. Lett. **83**, 1131 (1999)

[47] R. Hubele, A. LaForge, M. Schulz, J. Goullon, X. Wang, B. Najjari, N. Ferreira, M. Grieser, V. L. B. de Jesus, R. Moshammer, K. Schneider, A. B. Voitkiv, and D. Fischer, Phys. Rev. Lett. **110**, 133201 (2013)

[48] M. F. Ciappina, M. S. Pindzola, and J. Colgan, Phys. Rev. A **87**, 042706 (2013)

[49] T. Kirchner, N. Khazai, and L. Gulyás, Phys. Rev. A **89**, 062702 (2014)

[50] H. R. J. Walters, and C. T. Whelan, Phys. Rev. A **89**, 032709 (2014)

[51] L. Gulyás, S. Egri, and T. Kirchner, Phys. Rev. A **90**, 062710 (2014)

[52] M. D. Śpiewanowski, L. Gulyás, M. Horbatsch, and T. Kirchner, Phys. Rev. A **93**, 012707 (2016)

[53] R. Hubele, M. Schuricke, J. Goullon, M. Lindenblatt, N. Ferreira, A. Laforge, E. Brhl, V. L. B. de Jesus andD. Globig, A. Kelkar, D. Misra, K. Schneider, M. Schulz, M. Sell, Z. Song, X. Wang, S. Zhang, D. Fischer, Rev. Sci. Instr. **86**, 033105 (2015)

[54] A. C. LaForge, R. Hubele, J. Goullon, X. Wang, K. Schneider, V. L. B. de Jesus, B. Najjari, A. B. Voitkiv, M. Grieser, M. Schulz, D. Fischer, J. Phys. B: At. Mol. Opt. Phys. **46**, 031001 (2013)

[55] D. H. Madison, D. Fischer, M. Foster, M. Schulz, R. Moshammer, S. Jones, and J. Ullrich, Phys. Rev. Lett. **91**, 253201 (2003)

[56] U. Chowdhury, M. Schulz, and D. H. Madison, Phys. Rev. A **83**, 032712 (2011)

[57] M. Gell-Mann, and M. L. Goldberger, Phys. Rev. **91**, 398 (1953)

[58] D. S. F. Crothers, J. Phys. B: At. Mol. Phys. **15**, 2061 (1982)

[59] S. Jones and D. H. Madison, Phys. Rev. A **65**, 052727 (2002)

[60] A. Dorn, A. Elliott, J. Lower, E. Weigold, J. Berakdar, A. Engelns, and H. Klar, Phys. Rev. Lett. **80**, 257 (1998)

[61] A. E. S. Green, D. L. Sellin, and A. S. Zachor , Phys. Rev. **184**, 1 (1969)

[62] P. P. Szydlik, and A. E. S. Green, Phys. Rev. A **9**, 1885 (1974)

[63] R. H. Garvey, C. H. Jackman, and A. E. S. Green, Phys. Rev. A **12**, 1144 (1975)

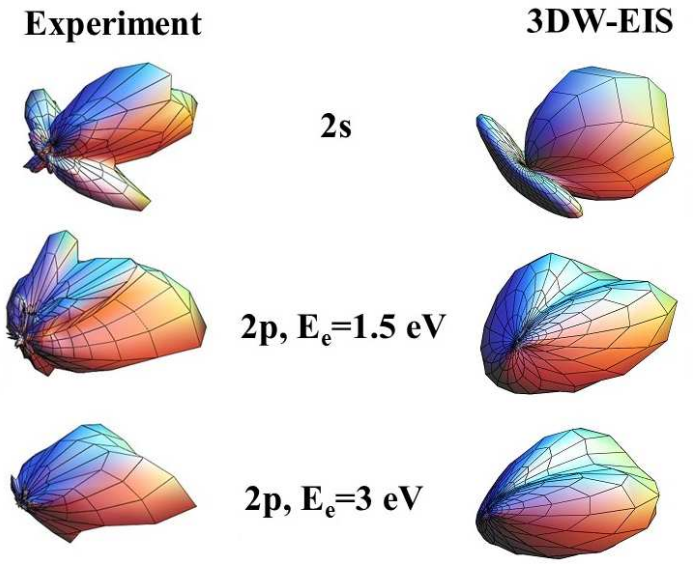

FIG. 1. (Color online) Comparison of experimental and theoretical 3DW-EIS results in 3-dimensions for 24 MeV O^{8+} ionization of the $2s$ and $2p$ states of lithium. For $2s$, E_e= 1.5 eV and the momentum transfer is q= 1 au. For $2p$ and E_e= 1.5 eV, the momentum transfer is q= 0.3 au, and for $2p$ and E_e= 3 eV, the momentum transfer is q= 0.4 au.

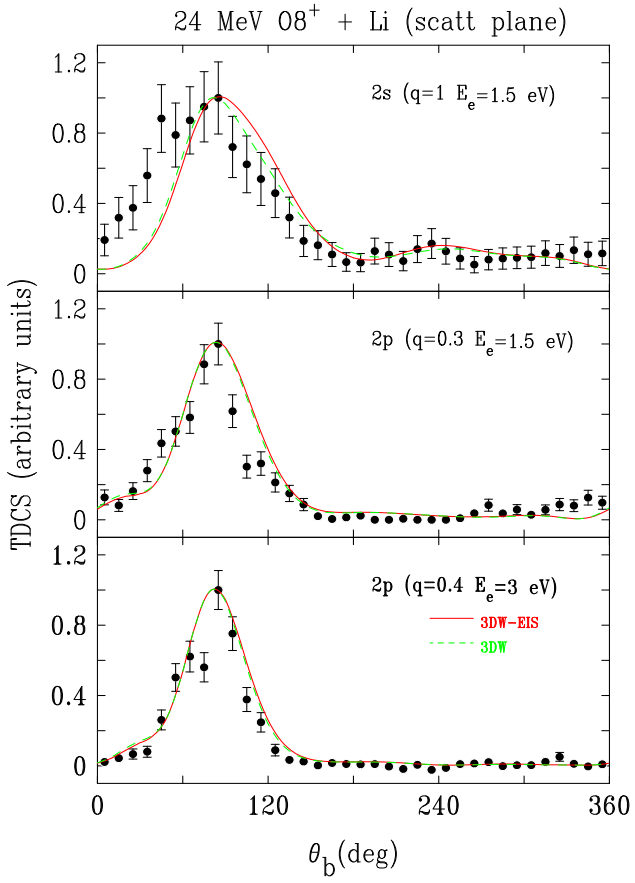

FIG. 2. (Color online) Comparison of experimental and theoretical results for 24 MeV O^{8+} ionization of the $2s$ and $2p$ states of lithium as a function of the ejected electron angle (θ_b) in the scattering plane. The projectile momentum transfer (q) and ejected electron energy (E_e) are indicated in each panel. The solid (red) results are 3DW-EIS and the dashed (green) lines are the 3DW results. The experimental and theoretical results are both normalized to unity at $\theta_b = 180^\circ$.

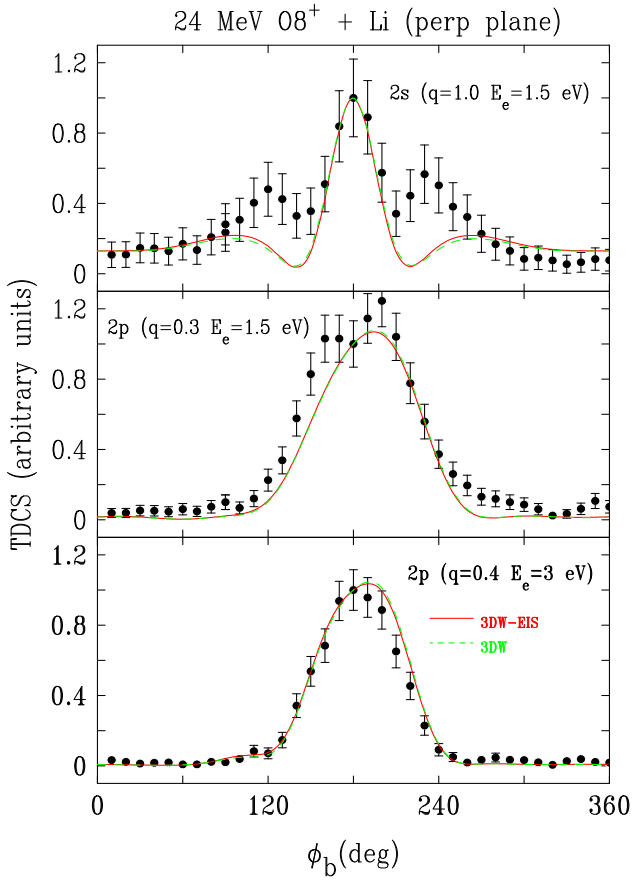

FIG. 3. (Color online) Comparison of experimental and theoretical results for 24 MeV O^{8+} ionization of the $2s$ and $2p$ states of lithium as a function of the ejected electron angle (θ_b) in the perpendicular plane. The projectile momentum transfer (q) and ejected electron energy (E_e) are indicated in each panel. The solid (red) results are 3DW-EIS and the dashed (green) lines are the 3DW results. The experimental and theoretical results are normalized the same as the scattering plane.

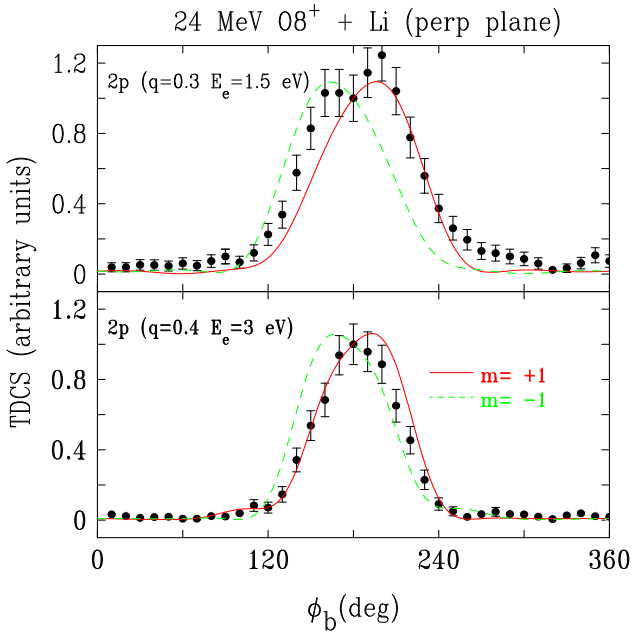

FIG. 4. (Color online) Comparison of experimental and theoretical $m = \pm 1$ results for 24 MeV O^{8+} ionization of the $2p$ states of lithium as a function of the ejected electron angle (θ_b) in the scattering plane. The projectile momentum transfer (q) and ejected electron energy (E_e) are indicated in each panel. The solid (red) lines are 3DW-EIS $m = +1$ results and the dashed (green) lines are the 3DW-EIS $m = -1$ results.

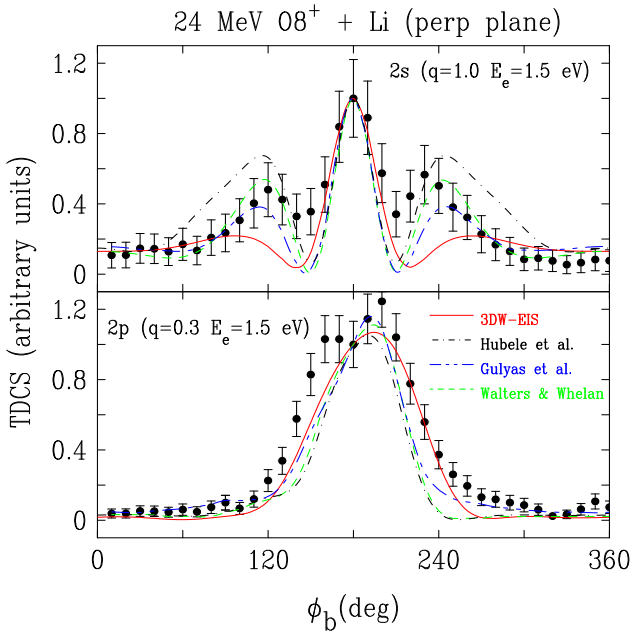

FIG. 5. (Color online) Comparison of 3DW-EIS results with previous theoretical calculations. The projectile momentum transfer (q) and ejected electron energy (E_e) are indicated in each panel. The solid (red) lines are 3DW-EIS results, dashed-dot (black) curves are the results of Hubele *et al.* [47], the long dash-two short-dash (blue) curve are the results of Gulyás *et al.* [51], and dashed (green) curve are the results of Walters and Whelan [50].

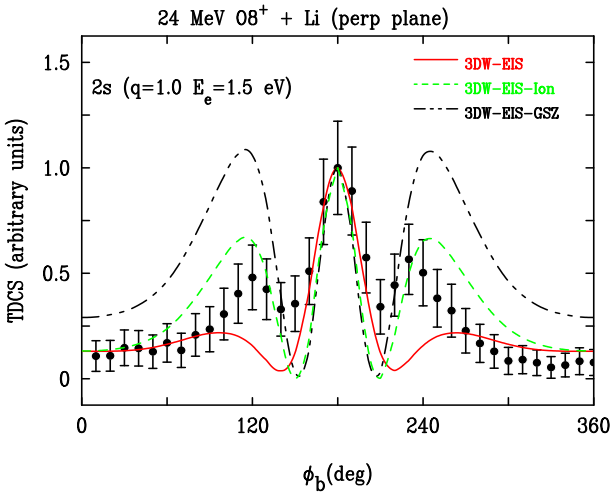

FIG. 6. (Color online) Comparison of 3DW-EIS results using different approximations for the NN interaction. The solid curve (red) has no NN in the perturbation, dashed (green) uses the bare ion potential and the long dash - two short dash (black) uses the GSZ screening approximation

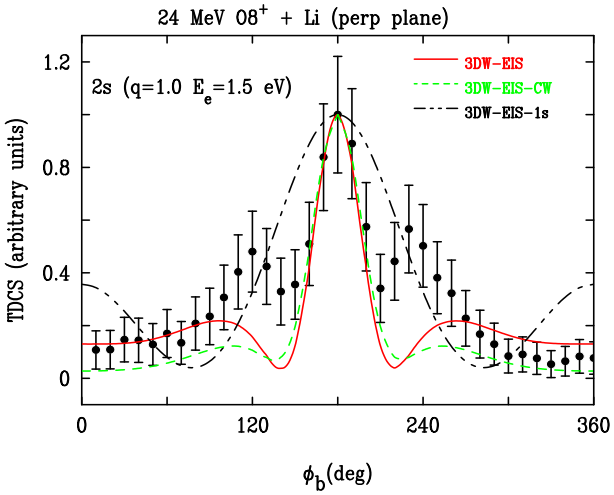

FIG. 7. (Color online) Comparison of different types of 3DW-EIS calculations. The solid curve (red) is the normal, dashed (green) uses a Coulomb wave for the ejected electron and the long dash - two short dash (black) 1s bound state wavefunction instead of a 2s.